Crossover behavior in a communication network

Brajendra K. Singh* and Neelima Gupte†
Department of Physics, Indian Institute of Technology, Madras, Chennai 600 036, India
(Received 2 December 2002; revised manuscript received 29 September 2003; published 30 December 2003)

We address the problem of message transfer in a communication network. The network consists of nodes and links, with the nodes lying on a two-dimensional lattice. Each node has connections with its nearest neighbors, whereas some special nodes, which are designated as hubs, have connections to all the sites within a certain area of influence. The degree distribution for this network is bimodal in nature and has finite variance. The distribution of travel times between two sites situated at a fixed distance on this lattice shows fat-fractal behavior as a function of hub density. If extra assortative connections are now introduced between the hubs so that each hub is connected to two or three other hubs, the distribution crosses over to power-law behavior. Crossover behavior is also seen if end-to-end short cuts are introduced between hubs whose areas of influence overlap, but this is much milder in nature. In yet another information transmission process, namely, the spread of infection on the network with assortative connections, we again observed crossover behavior of another type, viz., from one power law to another for the threshold values of disease transmission probability. Our results are relevant for the understanding of the role of network topology in information spread processes.

DOI: 10.1103/PhysRevE.68.066121 PACS number(s): 89.75.Hc

I. INTRODUCTION

In recent years there has been an unprecedented rise of interest in the study of networks and their properties [1,2]. These networks can be basically regarded as a collection of nodes linked by edges. The nodes represent individual entities, while the edges represent interaction between any pair of nodes in the network. Many natural systems, as well as engineered systems, can be represented by such networks. Some examples of such networks are found at large spatial scales, e.g., the internet or the power grid, while others are at single organismic levels, e.g., metabolic pathways [1–3]. The structure and connectivity properties of such networks and the capacity and degree of connectivity of their nodes have important consequences for processes which occur on the network. Some examples of such processes are message transfer in communication networks, the spread of infectious diseases in social networks, the spread of computer viruses in computer networks, and avalanche spread in load-bearing networks [4–9]. Such network studies have been seen to have potential applications in different fields of science and technology, including epidemiology and ecology.

Several different classes of network topologies have attracted recent interest. These include small-world (SW) network models which have short paths between any two nodes and highly clustered connections [10], and their variants [4,7], generalized families of small-world networks [11], and scalefree (SF) networks which incorporate the existence of ''hubs,'' viz., nodes with many more connections than the average node [12,13]. There have also been attempts to characterize the topology of natural networks, using measures such as average path lengths, clustering coefficients, degree distributions, and the existence of ''network motifs'' [14], viz., patterns of interconnections occurring in complex networks at numbers that are significantly higher than those in randomized networks.

It is known that the nature of the network topology significantly affects the manner in which spread processes occur on networks. A striking example of this was found by Kleinberg, where a decentralized algorithm was able to find very short paths (resulting in very short delivery times for messages) for a two-dimensional network where long-range connections followed the inverse square law. Another example where the topology of the network had a significant role to play is in the spread of computer viruses. It was seen that computer viruses can spread on the SF networks with zero transmission threshold [15,16] and that networks of differing topologies have differing degrees of vulnerability to attack [17–19] and different extents of error tolerance. The importance of such studies from the point of view of applications is obvious.

In this paper, we set up a communication network on a two-dimensional lattice. Communication networks based on two-dimensional lattices have been considered earlier in the context of search algorithms [11], as well as in the context of traffic on lattices with hosts and routers [20–24]. The lattice we consider in this paper has two types of nodes, viz., regular nodes and hubs. Each regular node on the lattice has connections with its nearest neighbors, whereas some special nodes, which are designated as hubs, have connections to all the sites within a certain area of influence. Thus, nodes falling within the influence area of a hub can directly interact with the hub, or vice versa. The degree distribution of this network is bimodal and has finite variance. We examine two distinct spread processes on this lattice network as functions of hub density. The distribution of travel times for a message transmitted between a fixed pair of sites for this lattice shows fat-fractal behavior as a function of hub density. If extra connections are now introduced between the hubs so that each hub is connected to two or three other hubs, the distribution crosses over to power-law behavior. The end-to-end short cutting of hubs whose influence areas overlap also in-

*Email address: braj@chaos.iitm.ernet.in
†Email address: gupte@chaos.iitm.ernet.in

duces crossover, but this is much milder in nature. We also examined the process of disease transfer on this network, a process that differs from message transfer in the fact that it is a probabilistic process and not a directed transfer between a source and a target. Here again the transmission threshold plotted as a function of hub density crossed over from one type of power-law behavior to another on the introduction of two extra connections per hub.

In Sec. II we set up the model of the communication network. In Sec. III we discuss the problem of directed message transfer between source and target nodes on this network. In Sec. IV we discuss the spread of information as a random process as in the spread of disease. The last section summarizes our conclusions.

II. THE MODEL

As stated in the Introduction, the proposed network is a two-dimensional lattice of nodes where every node is connected to its nearest neighbors. A certain fraction of the total nodes are designated as hubs, viz., as nodes which have connections to all nodes within their area of influence, where the area of influence is defined as a square area around the hub, which accommodates $(2k+1)^2$ nodes, including the hub node, k being the distance in lattice units (LU) from the hub to the outermost node in any principal direction within the square. All nodes within the influence area of a hub are termed its constituent nodes. A schematic representation of a hub node is shown in Fig. 1. These hubs are randomly chosen on the lattice maintaining a minimum distance d_{min} between any pair of hubs. This parameter (d_{min}) controls the extent of overlap between the influence regions of the hubs. See the two hubs "*d*" and "*e*" in Fig. 1. The distance between them is unity, and their influence regions are maximally overlapped. As the number of hubs on the lattice goes up, the number of connections that a constituent node can have also goes up, as it increasingly acquires links with more hubs because of the overlapping of the influence regions of the hubs. Thus the model takes into account the fact that local clustering in a geographical neighborhood can occur for many realistic models.

The hubs in this model connect to a fixed number of nodes, as in many realistic environments, where the number of links that can attach to a given hub is limited by the number of ports to the hub. We examine the influence that the presence of hubs exerts on the connectivity distribution of the network. In the absence of the hubs each node has the same degree of connectivity and the degree distribution (where the degree of a node is the number of nodes it is connected to) is a δ function with a single peak at 4. However, the introduction of hubs leads to completely different connectivity patterns for the network. Due to the presence of hubs, the connectivity of the nodes ranges from 4 (for the regular nodes) to $(2k+1)^2-1$ (for the hubs). The degree of the constituent nodes lies between the two extremes, being equal to $C+4$ where the constituent node lies in the overlapping influence area of C hubs. The degree of the constituent nodes is thus a function of the hub density, which controls the extent to which the influence areas of different hubs

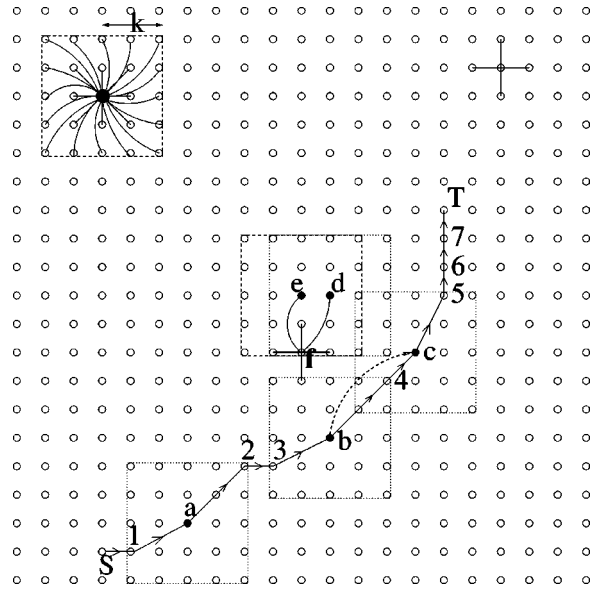

FIG. 1. A two-dimensional lattice of 21×21 nodes. The top left corner shows a hub (a filled circle) which is directly connected to all its constituent nodes within the square shown by the dashed lines. The side of the square is approximately equal to $2k$, shown for $k=2$. The square shown is called the influence area of a hub. A regular node that is neither a hub nor a constituent node has four edges connected to its nearest neighbors (shown in the top right corner). A typical path between a source node *S* and a target node *T* is shown with the labeled sites. Note that it passes through three hubs, namely, *a*, *b*, and *c* (filled circles). After scheme I the distance between *b* and *c* is covered in one step. The shortcut is shown by the dashed arrow from *b* to *c*.

overlap. Figure 2 shows a typical distribution of the degree of connectivity of nodes of all types for a lattice of size 100×100, $k=3$, $d_{min}=1$, and the hub density is 4.0%. As expected, there are two peaks in the distribution: one, a sharp one, at $(2k+1)^2-1$ corresponding to the degree of connectivity of the hubs, and the other around 4 (the degree of the regular sites) with a spread around the value. This spread comes from the constituent nodes of hubs with overlapping regions of influence. It is clear that the degree distribution does not fall into either of the two broad classes of networks—the SW and SF net-

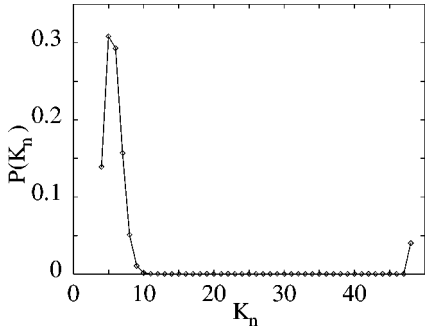

FIG. 2. A typical connectivity distribution for the proposed communication network. K_n gives the degree of connectivity of a node with K_n other nodes in the lattice. The lattice size is 100×100, $k=3$, and the hub density is 4.0%.

works. It also differs from the connectivity patterns of the random graphs. (See Ref. [13] for the connectivity distributions for the SW and SF networks as well as those of random graphs, and Refs. [25,26] for scalefree models with local clusters and geographic separation.) The variance in the degree distribution of our model is finite unlike that in the case of scalefree networks where the variance is infinite. This fact can have very important consequences for information spread processes on a network. The importance of the variance in the spread of disease has already been noted in the case of scalefree networks. It is therefore interesting to investigate spreading processes in models such as ours which do not have infinite variance, and to compare them with spreading processes seen in the case of other networks, e.g., scalefree networks with and without local clustering in a geographic neighborhood.

We now study two types of communication problems in this network, viz., the problem of message transfer and that of the spread of infectious disease.

III. THE PROBLEM OF MESSAGE TRANSFER

We study the transfer of a message from an arbitrary source node to an arbitrary target node on the lattice. Each (ordinary) node transfers the message to the node nearest to it in the direction which will minimize the distance from the current message holder to the target. When any constituent node of a hub is the current message holder, then the node directly sends it to the hub. The lattice distance between the sender node and the hub is just one hop because of direct communication between them, thereby speeding up the process of message transmission. If the hub is the current message holder the message is forwarded to one of the constituent nodes within its influence area, the choice of constituent node being made by minimizing the distance to the target. Thus the presence of hubs on the lattice increases the message transfer speed along the path, and the total travel time depends primarily on how many hubs fall on the path for the given influence radius k. A typical travel path for such a lattice is shown in Fig. 1 and is also indicated by the label *"O"* in Fig. 3.

A. Speed enhancement schemes

It is clear that the presence of hubs on the lattice makes the process of the message transfer faster than the situation when there are no hubs. However, there is further scope to enhance the speed of transmission. Here we discuss two speed enhancing schemes which can be practically applicable to the communication process.

Scheme I. Whenever there is an overlap between influence areas of hubs, then the message is transferred from the first hub to second, then to the third, and so on. Intermediate constituent nodes do not participate in the process of message transfer towards the target. For example, if there is an overlap between the influence regions of two hubs, namely, *A* and *B*, along the path, then after receiving the message the first recipient constituent node of *A* directly forwards it to its hub *A*, which directly sends it to *B*, from which the message is subsequently sent to the second recipient constituent node of *B*. The second recipient node of *A* and the first recipient node of *B* here do not take part in the message transfer. This scheme, in essence, introduces a single short cut for two hops per pair of overlapped hubs in the travel path. A typical travel path for this scheme is indicated by the label *"I"* in Fig. 3. As we will see in the following section, the introduction of this scheme, leads to an increase in the travel speed and a reduction in the message delivery time. However, the actual reduction in travel time for a given value of k crucially depends on the extent of overlap, which in turn depends on the minimum distance d_{min} between hub nodes, as well as on the hub density. For example, for the travel path *I* of Fig. 3, only one pair of hubs overlap so that the reduction in travel time is just one unit.

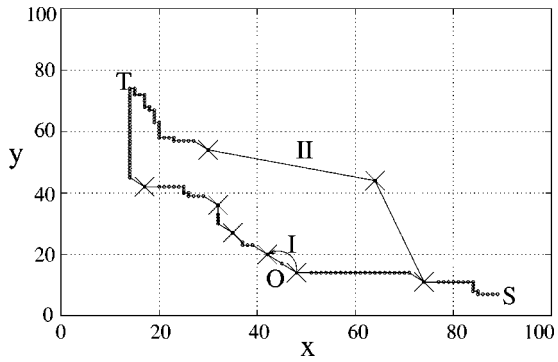

FIG. 3. Typical travel paths between source *S* and target *T*. The label *"O"* indicates a path on the original lattice, *"I"* a path on the scheme I lattice and *"II"* indicates a path when the lattice was modified by the scheme II. The lattice distance between for the source and target node is 142 LU. The lattice size is 100×100, $k=3$, and the hub density is 0.5%.

The minimum distance between any pair of hubs, d_{min}, decides the range of overlap between the influence regions of the hubs in our network. For any choice of k at a fixed hub density, a hub distribution with $d_{min}=1$ on the lattice guarantees that the separation between any pairs of hubs is equal to or greater than 1. It is easy to see that the areas of influence of a pair of hubs with $d_{min}=1$ have the maximum overlap. See Fig. 1. On the other hand, $d_{min}=2k+1$ for a given k results in no overlapping hubs on the lattice. Scheme I cannot be implemented for this case. Distributions of hubs with other intermediate values of d_{min} have overlaps that lie between the two extremes.

Scheme II. In the second scheme to speed up the communication process we connect individual hubs with a few (in this paper, typically two or three) other hubs selected at random. These connections, where nodes preferentially get connected to nodes having a similar degree of connectivity in the network, are called assortative connections [27,28]. Under this scheme, when a hub becomes the current message holder, it first tries to send the message through one of its assortative linkages to another hub which, among all acquaintances of the hub, happens to be the nearest to the target. If the current message holder hub cannot utilize its assortative linkages because of unsuitable locations of the end-point hubs, the message is sent to the constituent node nearest to the target. A typical travel path between

source "*S*" and target "*T*" is indicated by the label "*II*" in Fig. 3. Here the Manhattan distance D_{st} between source and target is 142, where the Manhattan distance is defined as $D_{st}=|is-it|+|js-jt|$ and (is,js) and (it,jt) are the coordinates for the source and the target, respectively. However the travel path labeled *II* needs just 50 steps to travel between the source and target. In comparison, the path labeled *O* needs 95 steps and that labeled *I* needs 94 steps.

The simulations are carried out as follows. Two nodes are selected as the source and the target at random from a lattice of a given size. The distance between them, denoted by D_{st}, is chosen to be the Manhattan distance. The number of steps required in delivery of the message from the source to the target are counted for 50 realizations of hubs for a given hub density. Then, the two nodes, i.e., the source and the target nodes, are replaced by two other nodes selected at random from the lattice, keeping D_{st} unchanged. Again the message transmission steps are counted for the same number of hub realizations. This is repeated for 1000 pairs of source and target nodes for a particular hub density. It should be noted that the order of averaging makes no difference. The value of d_{min} and k used throughout the paper are 1 and 3, respectively, unless otherwise specified.

B. Crossover behavior

The average travel time between a source and a target fixed distance apart is a good measure of the efficiency of the network for message transmission. This clearly depends on the density of hubs in the network, as well as on the way in which these hubs are connected. We study the behavior of average travel times as a function of hub density for a fixed Manhattan distance D_{st} between source and target. Our simulations were carried out for a lattice of 500×500 nodes, $D_{st}=712$, for the original networks as well as the networks modified by schemes I and II. Figure 4 shows the dependence of the average travel times, t_{avg}, as a function of hub density for the original networks (diamonds) for $d_{min}=1$. The average travel times decrease exponentially as the hub density increases. The data can be fitted well by the exponential function [29] $f_1(x)=Q_1\exp[-A_1x^{\alpha_1}]$, where $\alpha_1=0.4482$, $A_1=0.0142$, and $Q_1=730$. This can be rewritten in the form $f_1(x)=Q_1\exp[-(x/x_0)^{\alpha}]$, where x_0 is $(1/A_1)^{1/\alpha_1}$ and has the approximate value 13 259. Expanding this we get $f_1(x)=Q_1[1-X+(X^2/2!)-\cdots]$, where $X=(x/x_0)^{\alpha_1}$. Retaining terms to the lowest order, we see that the dependence of average travel times on hub density is given by $t_{avg}\approx Q_1(1-a\rho_{hub}^{\alpha_1})$, an instance of fat-fractal-like behavior. We plot the average travel times as a function of hub density on the same plot for the scheme I and scheme II networks. The behavior of t_{avg} in the case of scheme I networks (plus signs) is slightly different from that of the original network case, and the exponential function acquires a mild power-law correction. The data for scheme I networks is fitted well by a function $f_2(x)=Q_2\exp[-A_2x^{\alpha_2}]x^{-\delta}$, where $\alpha_2=0.46$, $A_2=0.0145$, $Q_2=735$, and $\delta=0.000\,05$. Scheme II networks show distinctly different behavior. The scheme II network data (boxes for two assortative connections and crosses for three assortative connections) can be fitted by a function $g(x)=Sx^{-\beta}$, where $\beta=0.2$ and S is a positive constant and thus shows power-law behavior. We note that the same power law fits both sets of scheme II data.

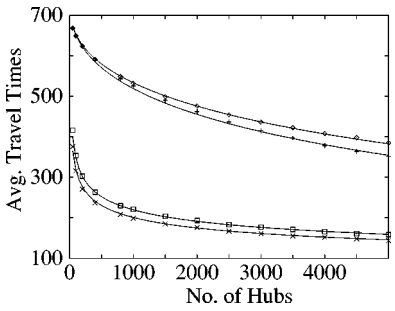

FIG. 4. A plot of average travel times, t_{avg}, vs number of hubs for the original network (diamonds), the scheme I network (plus signs), and the scheme II network (boxes) for two extra assortative connections and (crosses) three extra assortative connections per hub. Here, $d_{min}=1$. The best-fit line for the original network (diamonds) was given by the function $f_1(x)=Q_1\exp[-A_1x^{\alpha_1}]$, where $\alpha_1=0.4482$, $A_1=0.0142$, and $Q_1=730$. The behavior of t_{avg} for the scheme I network is slightly different and the exponential function needs a mild power-law correction given by $f_2(x)=Q_2\exp[-A_2x^{\alpha_2}]x^{-\delta}$, where $\alpha_2=0.46$, $A_2=0.0145$, $Q_2=735$, and $\delta=0.000\,05$. For scheme II networks the best-fit lines were given by the function $g(x)=Sx^{-\beta}$, where $\beta=0.2$ and $S=875$ (boxes), 800 (crosses).

Figure 5 shows the same data as Fig. 4 on a log-log plot. Here the drastic difference seen for the behavior of average travel times in the case of networks with scheme II operational compared to the other two networks can be clearly seen. The log-log plot of t_{avg} against the hub density is a straight line with slope $\beta=-0.2$. Thus $t_{avg}\approx\rho_{hub}^{-\beta}$ shows power-law behavior. It is again clear that the same power law is seen for the two scheme II cases. Thus the addition of a very small number of assortative connections per hub has induced a crossover to power-law behavior from the fat-fractal behavior seen in the nonassortative cases. The rate of fall-off of average travel times with increase in hub density is much faster for the assortative case even in the case of low

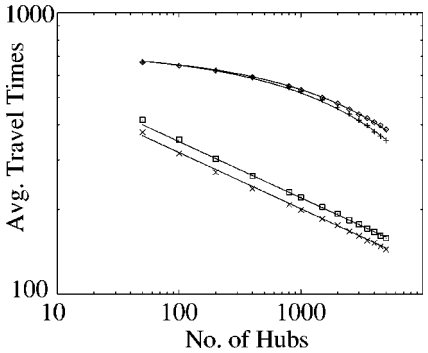

FIG. 5. The same data as in Fig. 4 is plotted on the log-log scale. These plots clearly show crossover in scaling behavior from the fat-fractal type seen for the original as well as the scheme I networks to the power-law behavior for the scheme II network. Note that the slope of the two parallel lines (the scheme II network) is -0.2.

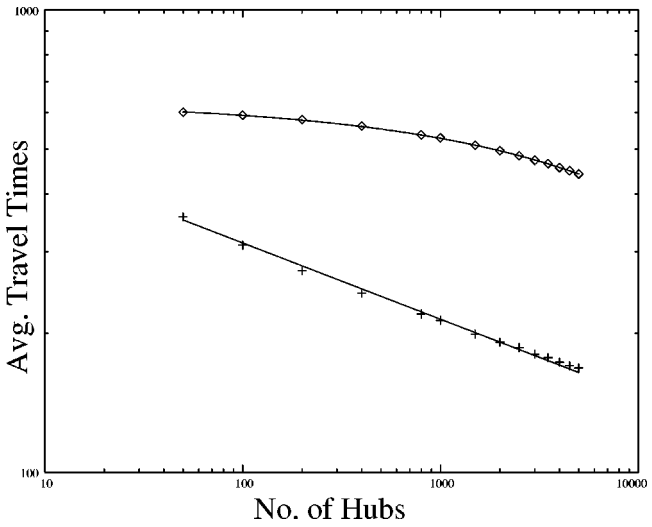

FIG. 6. The parameter values are the same as in Fig. 4 except for the following. First, the influence area for this figure is circular with a radius of k. Second, every node of the lattice network has been displaced by ± 0.1 from its earlier position as in Fig. 4. The functions for the fitted lines are $F(x)=635\exp(-0.0104x^{0.417})$ for diamonds (no assortative connections), and $G(x)=735x^{-0.165}$ for pluses (assortative connections).

hub densities. Thus the addition of assortative connections can increase the communication efficiency of networks without increasing the number of hubs in the network especially at low hub densities.

We note that the crossover from fat-fractal behavior to power-law behavior is insensitive to perturbations of the regular lattice geometry. We verified that up to 10% variation in the x and y locations in the location of the hub nodes makes no difference to the crossover behavior, although the numerical values of the exponents change. Similar perturbations to the location of all the nodes in the lattice also make no difference to the existence of the crossover. Changing the shape of the influence areas from square to circular regions introduces a variation in the degree of each hub, and also a perturbation to the overall degree distribution. We note that the crossover is robust to this change, as well. Figure 6 shows the behavior of the hub density for the lattice network with a perturbed node distribution with a circular influence area for the hubs, with all other parameters as in Figs. 4 and 5. It is clear that the crossover is completely stable to perturbation. The travel times can be fitted by the functions $F(x)=635\exp(-0.0104x^{0.417})$ for the perturbed lattice with no assortative connections, and by the function $G(x)=735x^{-0.165}$ for the perturbed case with assortative connections. We note that the exponent β now takes the value 0.165 from the value 0.2 seen earlier, and the power-law α_1 changes to 0.417 from the value 0.4482, but the constant A_1 barely changes from $A_1=0.0142$ to $A_1=0.0104$, a change in the third place after the decimal. Thus the fat-fractal behavior of the type $C(1-x_1^{\alpha})$ remains unaltered due to the perturbation as does the power-law behavior for the network with assortative connections. Thus, the crossover is robust to perturbation.

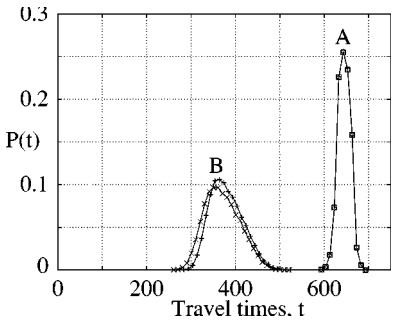

FIG. 7. The distributions of paths in terms of travel times for $D_{st}=712$ on a lattice of 500×500. The distributions shown are for $d_{min}=1$. The curve indicated by "A" is for a total of 100 hubs and the curve "B" for a total of 5000 hubs. Plots with diamonds and plus signs use the original network data while the boxes and crosses correspond to scheme I data.

C. Distribution of travel times

The probability distributions of travel times on the network for the three cases above can be seen in Figs. 7 and 8. It is clear that as hub densities increase, the peak shifts towards short travel times for the original network. When the message was transmitted using scheme I, the distribution changes very slightly with virtually no effect at low hub densities. However, when scheme II was operational, the distribution showed a marked change (see Fig. 8). The distributions of Fig. 7 (the original lattice and scheme I) are sharply peaked about a mean travel time and are symmetric about the mean whereas those of Fig. 8 show a much wider spread and are skewed. There is also a difference between the two distributions as shown in Fig. 8. At low hub densities the distribution is bimodal, whereas the bimodality is smoothed out at higher hub density. The right peak is reminiscent of the distribution for a lattice without any hub-to-hub connections at low hub density. Overall, the new distribution indicates that even sparse hub-to-hub connections are quite capable of inducing short paths at all hub densities. The distribution also shifts to lower values of travel times demonstrating the success of the short cutting assortative strategy (scheme II).

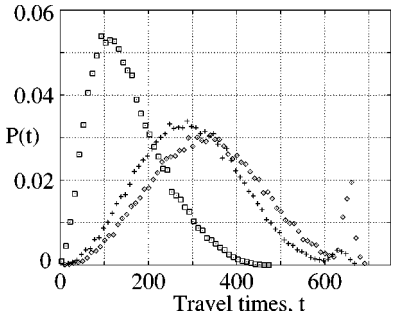

FIG. 8. The distributions of paths in terms of travel times for the same value of D_{st} when scheme II is operational. Diamonds are for a total of 100 hubs, plus signs for a total of 200 hubs, and boxes for a total of 5000 hubs. The lattice size, D_{st}, and d_{min} are the same as in Fig. 7. The distributions show bimodality (two peaks) at lower hub densities (diamonds and plus signs), and this bimodality disappears at higher hub densities (boxes).

IV. COMMUNICATION NETWORKS VERSUS SPREAD OF INFECTIONS

The message transfer problem discussed above involves the consistent directed transfer of a message towards a target. Each temporary message holder transfers the message, with probability one, in the direction which takes the message towards the target. Other types of processes of information spread such as the spread of computer viruses, infectious disease, rumors, popular fashions, etc. have distinctly different mechanisms of spread. These processes are not directed processes, and incorporate stochastic elements in the mechanism of spread. Hence communication networks which may be very efficient for information dissemination of the first type, may not be at all, or less suitable, for the second kind. In this section we examine the spread of an infection in a population of susceptible individuals for our network. The population contains both infected and susceptible individuals. The individuals constitute the nodes of the network, and social interactions among them constitute the edges by which infection can be transferred from one node to another. A similar model is also applicable to the spread of computer viruses. We consider a single point entry for infection in our study.

Many recent studies have focused on this kind of spread of diseases on networks [4–8,15,16]. A susceptible individual can get infected (with some probability) only when he directly or indirectly encounters infectious individuals in the population. The structure of the contact network has important implications for three things. The first is the rate at which an infection can spread across the network, the second is the transmission threshold, i.e., the smallest probability of infection with which the infection can spread to a significant fraction of the nodes of the network, and the third is the choice of an effective immunization strategy.

Recent studies of disease spreading viruses or computer virus spreads on networks of the SF type show that the possibility of these viruses being persistent in the population, and of their being resurrected causing repeated epidemics, is almost independent of any transmission threshold [15]. Thus, in the case of the SF networks, all that is needed for the infection to spread throughout the population is the occurrence of a single-time point entry of the infection into the population. Since it has been argued that in the case of sexually transmitted diseases, particularly that of the HIV/AIDS infection, the underlying contact networks have scalefree character [30], this result also has implications for the spread of such diseases. However, the existence of a vanishing threshold in the case of human disease does not fit well with the conventional epidemiologist's viewpoint. The infinite variance of the node connectivity in the SF network has been identified as the causative agent for the vanishing threshold seen in such networks [27,31,32]. Thus, though traditional epidemiology acknowledges the importance of heterogeneity in the rapid spatial spread of diseases such as HIV/AIDS, the extreme heterogeneity seen in SF networks may not make them good candidates for modeling other kinds of infection in human or animal populations, where social contacts generally do not conform fully with the SF characteristic [3,33].

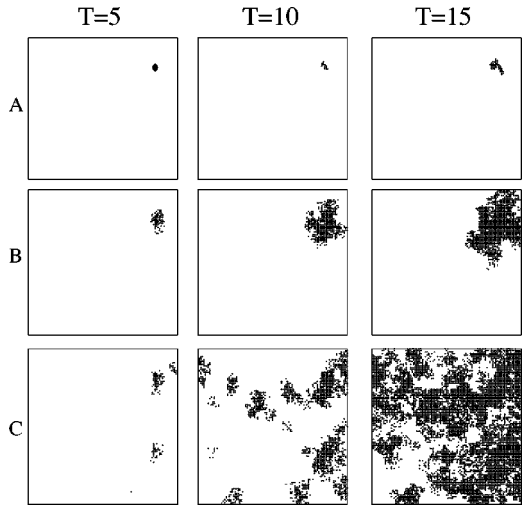

FIG. 9. The spread of infection on a lattice with no hubs (top row, labeled A), on a lattice with hubs (middle row, labeled B), and a lattice with hubs with two assortative connections (bottom row, labeled C). Snapshots of the infection spread are taken at $t=5$, $t=10$, and $t=15$ (column labels) for each case. Here the infection probability $p=0.25$.

Hence the study of disease spread on other types of networks such as ours, which have finite variance, is important.

As mentioned above, network topologies also determine the choice of effective immunization strategies. Recent studies on immunization strategies for efficient and successful controlling of epidemics on SF networks have unanimously advocated the immunization of the most connected nodes [27,34,35]. The choice of immunization strategy would have to be quite different in the case of networks where the node-connectivity distribution is not of the SF type. Even in the case of SF networks, immunization strategies which concentrate on immunizing the most connected nodes do not take into account the finite probability that a few infected nodes, which may not be the most connected nodes on the network, might have long-range connections to new regions of the susceptible population, and hence, could transmit the disease to regions quite distant from their place of origin where a fresh epidemic can ensue. Our network, which incorporates geographic distance and local clustering, is useful for such a study.

We studied information spread via an infection process of the susceptible-infected-recovered type on this network. The process has the following features: (i) all nodes are equally susceptible, (ii) infection always starts from a single site, (iii) an infectious node can infect any of the nodes it is connected to with probability p, (iv) this transmission probability is the same, i.e., it has the value p irrespective of whether the infected node is a hub or an ordinary node, and (v) none of the nodes get infected twice. Also once a node becomes infected, it remains infected until it infects any one of its neighbors. Here we assume that within a typical infectious period an infected node certainly infects, at least, one susceptible node. In this study we restrict ourselves to a single episode of epidemic break.

We study the manner in which the infection spreads on a 100×100 node lattice. Figure 9 shows the manner in which the infection wave front from a single infected node travels

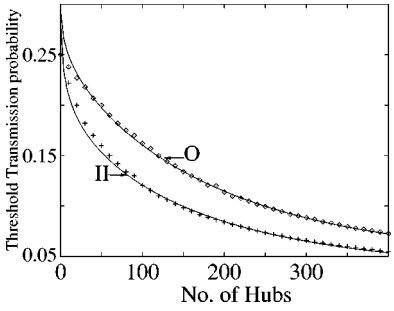

FIG. 10. The behavior of the threshold values of transmission probability p_{th} as the number of hubs increases. The best-fit line for plot I (for the original lattice) was drawn using the function $G(x) = D\exp[-Mx^{\zeta}](x+1)^{-\xi_1}+C_1$. The behavior for the lattices with two assortative connections per hub, shown by plot *II*, had to be fitted using another function $H(x)=D\exp[-Mx^{\zeta}](x+1)^{-\xi_2}+C_2$, where $D=0.25$, $M=0.0054$, $\zeta=0.975$, $\xi_1=0.065$, $\xi_2=-0.13$, $C_1=0.046$, and $C_2=0.036$.

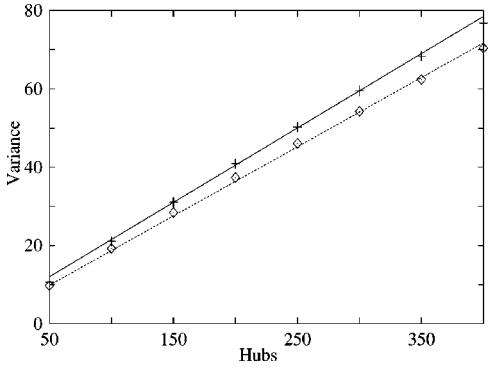

FIG. 11. The plot shows the variance in connectivity as a function of hub density for two cases—the original (diamonds) and scheme II networks (pluses). The lattice size is 100×100, $k=3$, and two assortative connections per hub for the strategy II case.

on a lattice with no hubs at $t=5$, $t=10$, and $t=15$ (top row, labeled A), on a lattice with hubs (middle row, labeled B) at the same time steps, and a lattice with hubs with two assortative connections (bottom row, labeled C). The rapid spread of infection in the bottom row can be very clearly seen. All the results in this section study infection spread for a 100×100 lattice with 400 hubs with $d_{min}=1$ and $k=3$. Other parameters are given in the figure caption. Each run is taken for 400 time steps.

A. Threshold behavior and crossover

The threshold value of the transmission probability p_{th} is a very crucial factor in the spread of disease. This quantity may depend on the structure and topology of the network. In the case of the spread of computer viruses on scalefree networks, the threshold value turns out to be zero, leading to very rapid spread of virus across such networks. In the case of immunological diseases, the threshold probability is finite. In this section we examine the behavior of this quantity for our networks as a function of the hub density.

The threshold transmission probability p_{th} is defined in the following way. For a fixed run of t time steps, the threshold value is defined to be the smallest value of the transmission probability for which at least 50% of the total number of susceptible sites are infected by half the run. Figure 10 shows the behavior of p_{th} against the number of hubs. The diamonds show the observed behavior for the original network and the plus signs the behavior for the scheme II network when there are two assortative (hub-to-hub) connections per hub. The data for the original network could be fitted using a function $F(x)=D\exp[-Mx^{\zeta}](x+1)^{-\xi_1}+C_1$. The behavior for the scheme II networks (plus signs) was somewhat different and had to be fitted using another function, $G(x)=D\exp[-Mx^{\zeta}](x+1)^{-\xi_2}+C_2$, where $D=0.25$, $M=0.0054$, $\zeta=0.975$, $\xi_1=0.065$, $\xi_2=-0.13$, $C_1=0.046$, and $C_2=0.036$. Thus, there is a change in the scaling behavior of the threshold probability between the original network and the scheme II case. However this crossover is a gentle change from one power law to another, unlike the drastic change seen for the behavior of the average travel times for the same case. The change is more pronounced at low hub density as in the other case. The reason as to why the crossover is drastic in the case of the message transfer process but is more gentle in this case of the infection spread may lie in the fact that in the case of disease spread, the variance appears to be the crucial quantity which determines the threshold behavior. We plot the variance as a function of hub density in Fig. 11 for the original network (diamonds) as well as the network with assortative connections (plus signs). It is clear that there is very little difference between the behavior of the variance in the two cases. This appears to be the reason for the gentle crossover.

B. Immunization strategies

Studies of the SF networks have emphasized the importance of high connectivity nodes, and immunization strategies which immunize nodes of high connectivity are the most successful. However, nodes of moderate connectivity can open up new regions to the spread of infection if they are connected to nodes which are far away. Real-world epidemic events have always been affected by the long-distance movements of causative agents into susceptible regions [36]. Some recent studies [37,38] provide evidence for this. While studies of the SW networks take cognizance of the fact that long-range connections are important in the spread of information, it is never clear what fraction of connections in a small world are really long range, since the network is always stochastically generated using rewiring probabilities. Local clusters also play a crucial role in the spread of infection.

We try to isolate the contribution of long-range connections and that of the local clustering property in information and disease spread on the network with two assortative connections per hub by the use of different immunization strategies. Figure 12 plots the number of new infections as a

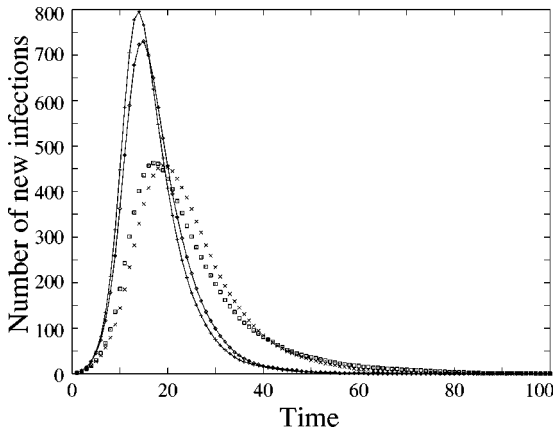

FIG. 12. The effect of immunization on the number of new infections when assortative bonds of length equal to or greater than 100 LU are immunized (diamonds), when hubs with assortative bonds of length greater than 100 LU are immunized (boxes, 117 hubs are immunized on an average in this case), and when 117 randomly chosen hubs are immunized (crosses). The plot also shows the number of new infections as a function of time (pluses) when the network has 400 hubs with two assortative connections per hub (the nonimmunized case). Here the infection probability $p = 0.25$.

function of time for this network. The plus signs indicate the number of new infections for the unimmunized network. The first immunization strategy immunizes the bonds which connect hubs separated by a distance greater than or equal to 100 LU (this is the Manhattan distance between the two hubs). For this lattice the average number of bonds of this type is about 17% of the total number of bonds. However, the hub itself is not immunized and can infect the local cluster. It is clear that the immunization of the long-range bonds causes the number of new infections to decrease (see plot with diamonds), and also causes the infection to spread more slowly. However, this effect is not pronounced. The second immunization strategy inoculates both the hubs which are connected by such long-range bonds so that no infection travels from the hub to any of the nodes connected to it. The number of new infections for this case is plotted with boxes in the same figure. It is clear that the rate of spread of infection slows down, the number of new infections peaks at a much lower value, and the distribution develops a long tail. The last plot, viz., the plot with crosses, shows the number of new infections as a function of time if the same number of hubs is immunized as in the last strategy, but if the hubs are randomly chosen (i.e., the hubs chosen do not necessarily have long-range bonds) it is interesting to note that there is very little difference between the two distributions. Thus, the local cluster which connects to other local clusters (not necessarily distant ones) appears to play a more crucial role in the spread of infection than the existence of long-range bonds. This is unlike the behavior seen earlier in the case of small-world networks. Thus immunization strategies which target arbitrary local clusters are as successful as those which target local clusters with additional long-range bonds. We observed this behavior at both low and high hub densities.

V. CONCLUSIONS

To summarize, in this paper we have studied information spread on a two-dimensional communication network with nodes of two types, ordinary nodes which are connected to their nearest neighbors and hubs which are connected to all nodes within a certain range of influence. The degree distribution for this lattice is bimodal in nature, and has finite variance. The average travel time for directed message transfer between source and target on this lattice shows fat-fractal behavior as a function of the hub density, however the introduction of a small number of assortative connections between the hubs (scheme II) induces a crossover to power-law behavior for this average travel time. In the case of scheme I networks, where a short cut was introduced between end-to-end hubs for consecutively overlapped hubs, a much milder crossover was seen. We also study the spread of infection on this network by the SIR process. The threshold level for the infection probability is finite for the networks with and without assortative connections, due to the fact that both networks have finite variance. However, the threshold level as a function of hub density shows crossover behavior when assortative connections are introduced when compared with the original network. However, this crossover is gentle in comparison to that observed for the average travel times for the directed message transfer for the same scheme II case. Thus, while network topology modifies the way in which information spreads on a network, the effect appears to be stronger for directed processes than for undirected processes. We also study the spread of infection and immunization strategies for this network, and conclude that local clustering plays as important a role as the existence of assortative connections in the rate of spread of infection. Thus assortative connections play a more crucial role in message transfer processes than in the spread of infection.

Our results can be of practical utility in a variety of contexts. In the case of directed message transfer, at low values of hub density, the average travel time between source and target can be reduced very rapidly by the introduction of very few assortative connections per hub. This is a very efficient way of reducing travel time without the introduction of new hubs. Long-range connections between hubs cut the travel time drastically in these cases. On the other hand, the existence of local clusters which can connect to other local clusters (not necessarily distant ones) seems to play an important role in the spread of infection. Thus immunization strategies which target local clusters appear to be called for. It is thus important to note that different elements of the network topology appear to be important for different types of information spread processes. We hope to explore this direction further in future work.

ACKNOWLEDGMENT

We thank CSIR, India, for partial support for this work.

[1] M.E.J. Newman, J. Stat. Phys. **101**, 819 (2000).
[2] Réka Albert and Albert-László Barabasi, Rev. Mod. Phys. **74**, 47 (2002).
[3] L.A.N. Amaral, A. Scala, M. Barthelemy, and H.E. Stanley, Proc. Natl. Acad. Sci. U.S.A. **97**, 11 149 (2000).
[4] M.E.J. Newman and D.J. Watts, Phys. Rev. E **60**, 7332 (1999).
[5] C. Moore and M.E.J. Newman, Phys. Rev. E **61**, 5678 (2000).
[6] M. Kuperman and G. Abramson, Phys. Rev. Lett. **86**, 2909 (2001).
[7] M.E.J. Newman, I. Jensen, and R.M. Ziff, Phys. Rev. E **65**, 021904 (2002).
[8] M.E.J. Newman, Phys. Rev. E **66**, 016128 (2002).
[9] T.M. Janaki and N. Gupte, Phys. Rev. E **67**, 021503 (2003).
[10] D.J. Watts and S.H. Strogatz, Nature (London) **393**, 440 (1998).
[11] J. Kleinberg, Nature (London) **406**, 845 (2000).
[12] Albert-László Barabasi and Réka Albert, Science **286**, 509 (1999).
[13] Albert-László Barabasi, Réka Albert, and Hawoong Jeong, Physica A **272**, 173 (1999).
[14] R. Milo, S. Shen-Orr, S. Itzkovitz, N. Kashtan, D. Chklovskii, and U. Alon, Science **298**, 824 (2002).
[15] R. Pastor-Satorras and A. Vespignani, Phys. Rev. Lett. **86**, 3200 (2001).
[16] Y. Moreno, R. Pastor-Satorras, and A. Vespignani, Eur. Phys. J. B **26**, 521 (2002).
[17] R. Albert, H. Jeong, and A.-L. Barabasi, Nature (London) **406**, 378 (2000).
[18] D.S. Callaway, M.E.J. Newman, S.H. Strogatz, and D.J. Watts, Phys. Rev. Lett. **85**, 5468 (2000).
[19] R. Cohen, K. Erez, D. ben Avraham, and S. Havlin, Phys. Rev. Lett. **86**, 3682 (2001).
[20] T. Ohira and R. Sawatari, Phys. Rev. E **58**, 193 (1998).
[21] R.V. Sole and S. Valverde, Physica A **289**, 595 (2001).
[22] H. Fuks, A.T. Lawniczak, and S. Volkov, Acm Trans. Model Comput. Simul. **11**, 233 (2001).
[23] H. Fuks and A.T. Lawniczak, Math. Comput. Simul. **51**, 103 (1999).
[24] It has been established that despite the regular geometry, traffic on the network reproduces the characteristics of realistic internet traffic [21].
[25] C.P. Warren *et al.*, Phys. Rev. E **66**, 056105 (2002).
[26] A.F. Rozenfeld, R. Cohen, and D. ben-Avrahem, Phys. Rev. Lett. **89**, 218701 (2002).
[27] Robert M. May and Alun L. Lloyd, Phys. Rev. E **64**, 066112 (2001).
[28] M.E.J. Newman, Phys. Rev. Lett. **89**, 208701 (2002); Phys. Rev. E **67**, 026126 (2003).
[29] Other values of d_{min} lead to similar behavior. The observed behavior can be fitted by $f_1(x)=Q_1\exp[-A_1x^{\alpha_1+(d_{min}-1)\epsilon}]$, where $\epsilon=0.005$ and other values are as in the text.
[30] F. Liljeros, C.R. Edling, L.A.N. Amaral, H.E. Stanley, and Y. Aberg, Nature (London) **411**, 907 (2001).
[31] Alun L. Lloyd and Robert M. May, Science **292**, 1316 (2001)
[32] Victor M. Eguiluz and K. Klemm, Phys. Rev. Lett. **89**, 108701 (2002).
[33] P. Holme, B.J. Kim, C.N. Yoon, and S.K. Han, Phys. Rev. E **65**, 056109 (2002).
[34] Z. Dezso and A.-L. Barabasi, Phys. Rev. E **65**, 055103(R) (2002).
[35] R. Pastor-Satorras and A. Vespignani, Phys. Rev. E **65**, 036104 (2002).
[36] M.E. Wilson, Emerg. Infect. Dis. **1**, 39 (1995).
[37] E. Ahmed, A.S. Hegazi, and A.S. Elgazzar, Int. J. Bifurcation Chaos **2**, 189 (2002).
[38] N.M. Ferguson, C.A. Donnelly, and R.M. Anderson, Science **292**, 1155 (2001).